1 Default protrusion at equilibrium temperature

1.1 Mesh convergence

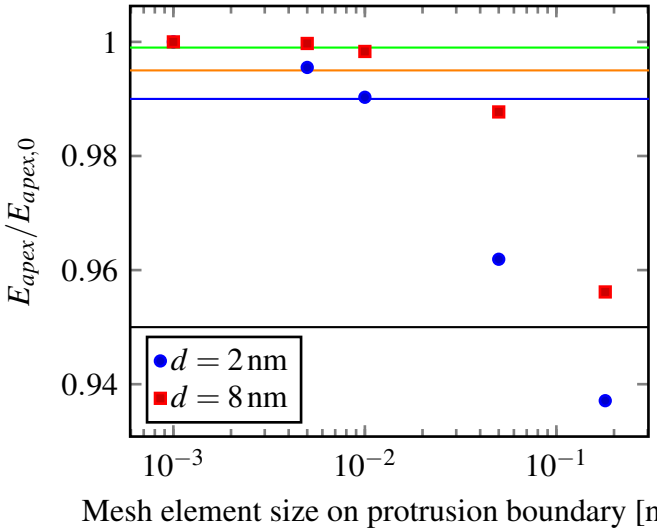

Figure 1: Mesh convergence. E_{apex} denotes the apex electric field for the given mesh size. $E_{apex,0}$ is the same value for the smallest mesh. The green and orange line correspond to a difference of 0.1% and 0.5% in the apex electric field, respectively. The corresponding error in current density can be found in the next figure (figure 2).

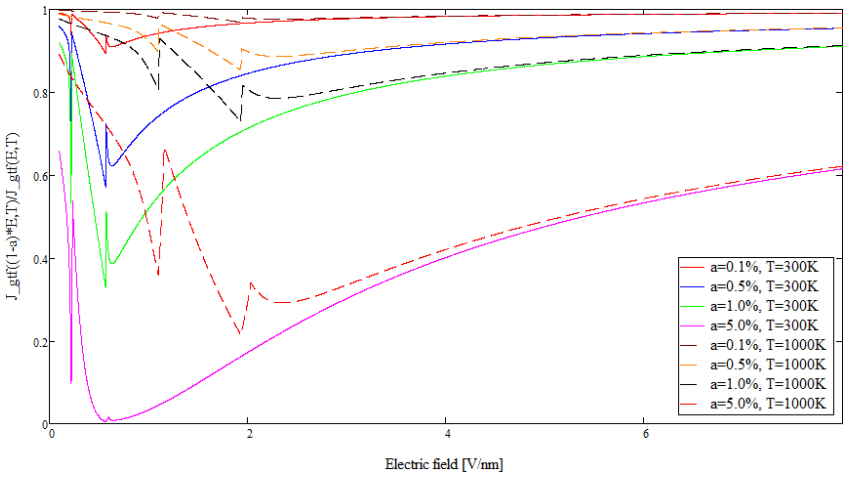

Figure 2: The error in current density $\frac{J_{GTF}((1-a)E,T)}{J_{GTF}(E,T)}$ due to the error a in the field at 300 K and 1000 K.

1.2 Temperature dependence on apex field

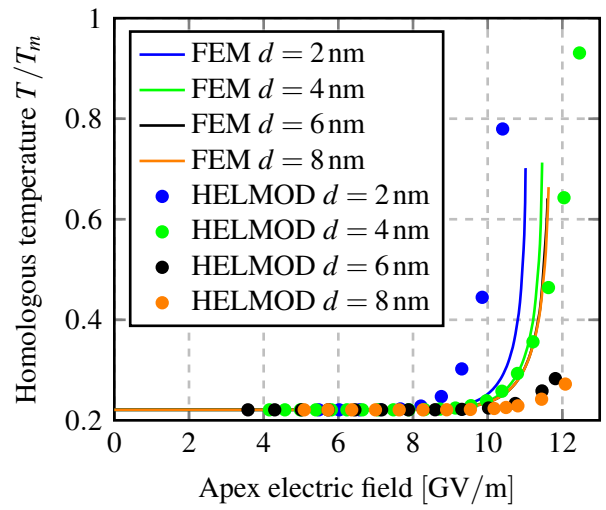

(a) $h = 5\,\text{nm}, d = 2\,\text{nm}$

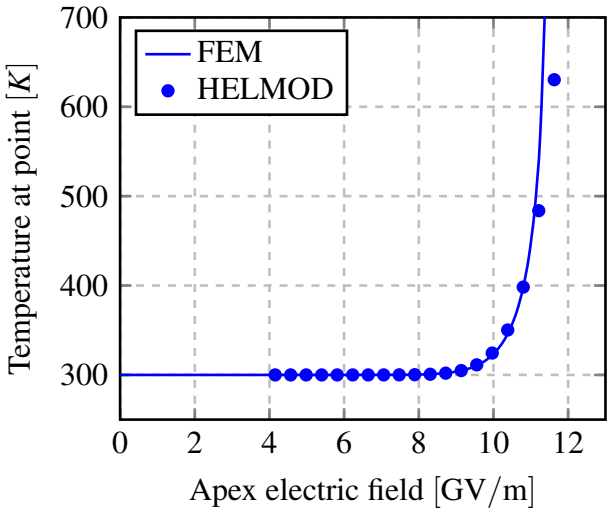

(b) $h = 5\,\text{nm}, d = 4\,\text{nm}$

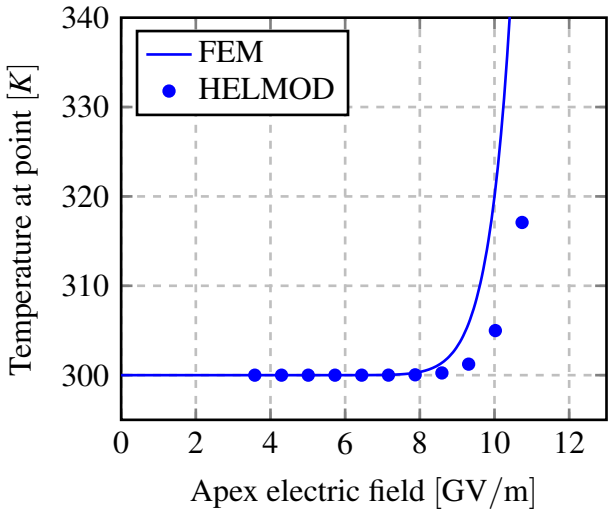

(c) $h = 5\,\text{nm}, d = 6\,\text{nm}$

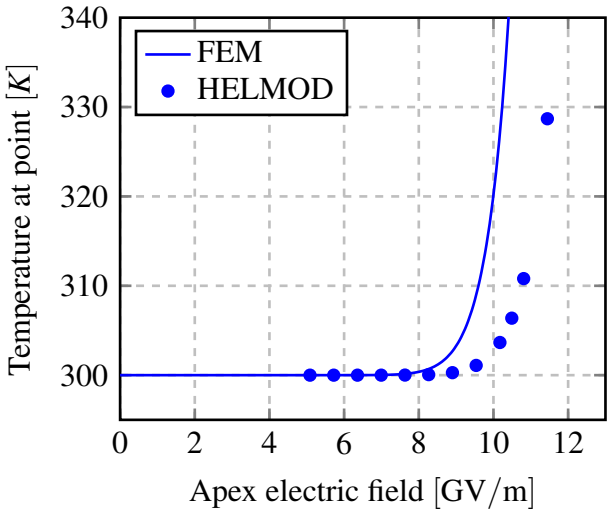

(d) $h = 5\,\text{nm}, d = 8\,\text{nm}$

Figure 3: The equilibrium temperature for the apex, center and the boundary point of the protrusion dependence on the apex local electric field for MD and FEM. For FEM, the mesh element size at the boundary was 0.005 nm (see figure 1) and the other elements were 0.18 nm.

2 Cylindrical protrusion at $T_0 = 300\,\mathrm{K}$

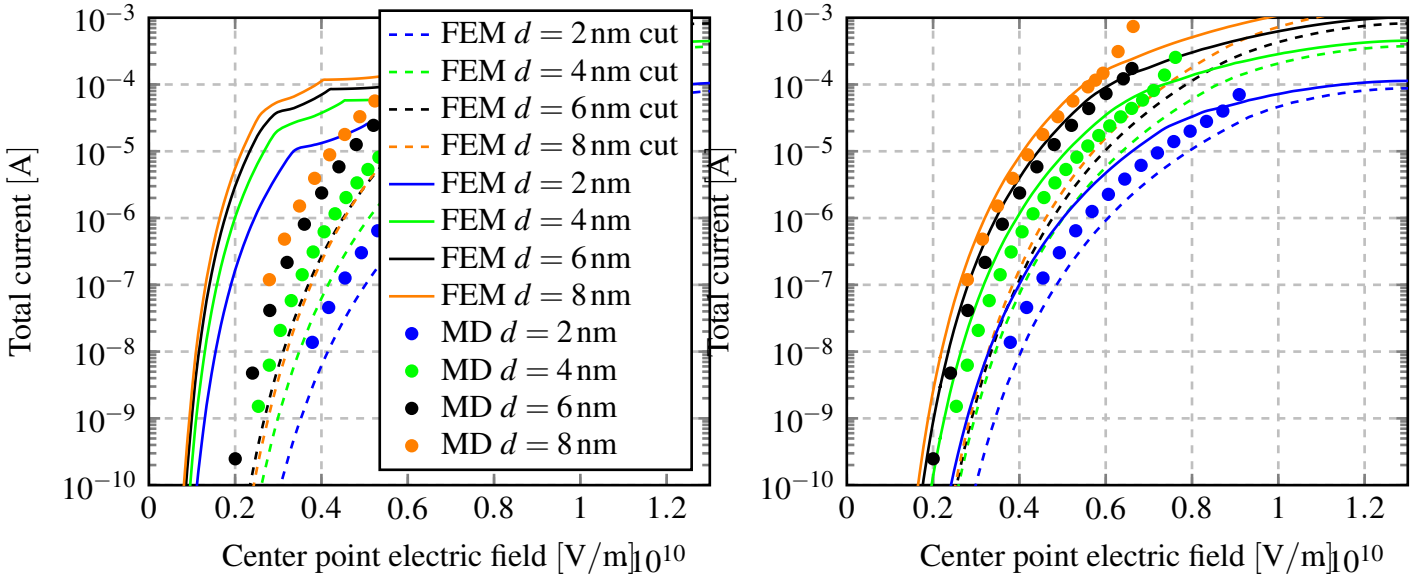

Figure 4: The total current from the top side of the cylindrical protrusion ($h = 5\,\mathrm{nm}$) versus the apex electric field for FEM and MD. The temperature is held constant at 300 K. Note that after about 11 GV/m, the GTFE (and also FN) equations are not valid. The used mesh is described in figure 5. For the MD values, the field has been capped at (14 V/nm ?), for FEM, the field was capped at 13 V/nm. The FEM values labeled as "cut" have the current ignored when $r > 0.9r_0$. In the left and right graph, the weak contraints are on and off, respectively.

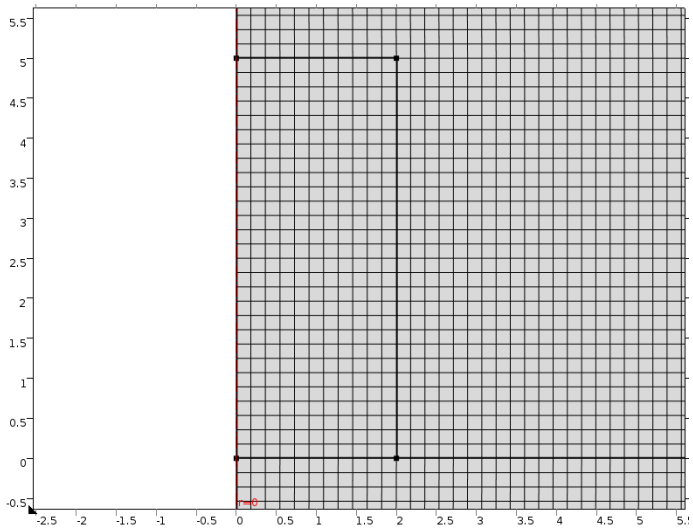

Figure 5: The protrusion has an uniform quadrilateral mesh, where each element's size is 0.18 nm.

3 Various results for constant temperature $T_0 = 300\,\mathrm{K}$

Note: The apex values found in this section do not correspond to the real apex point, but a point in close proximity. This is due to the COMSOL solver not finding the field correctly in the real apex point (and the values are unrealistic). The deviation in the used point from the real apex field is less than 0.2 %.

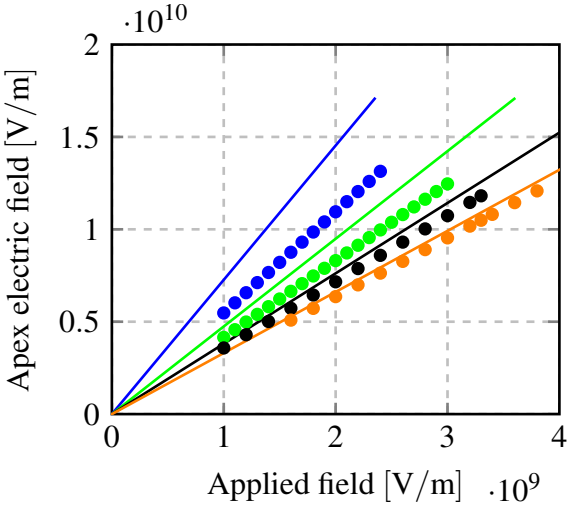

(a) Apex electric field

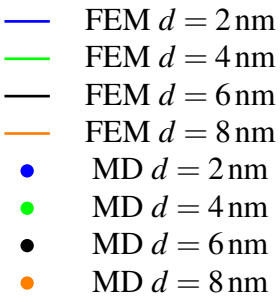

(b) Legend

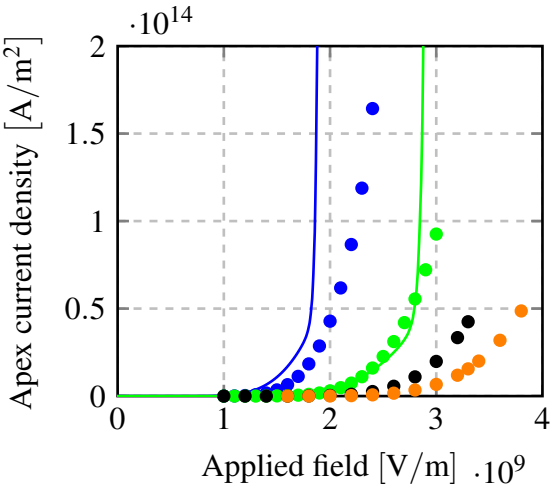

(c) Apex current density
(direct case for MD, i.e. the g_J value)

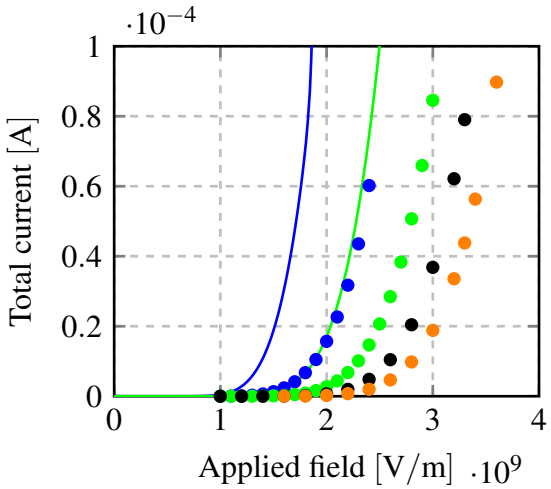

(d) Total current from emitter (only in $\hat{\mathbf{z}}$ direction for MD)

Figure 6: The local apex electric field (a), local apex (GTFE) current density (c) and the total current (d) dependence on applied electric field. Each of the dependences have been found for two protrusion sizes: ($h = 5\,\mathrm{nm}$, $d = 2\,\mathrm{nm}$) and ($h = 5\,\mathrm{nm}$, $d = 4\,\mathrm{nm}$). The dependencies have also been found with and without weak constraints (for the Diriclet boundary condition of potential on copper surface). The temperature was held constant at $T_0 = 300\,\mathrm{K}$. The used mesh was the same as in table 1.

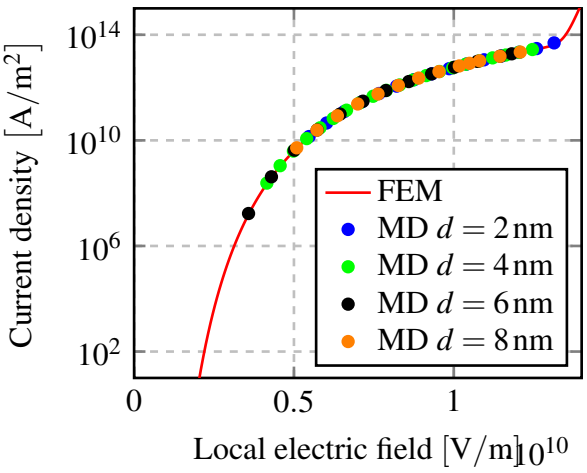

Figure 7: The current density dependence on local electric field for FEM and MD. The indirect values for MD have been found by diving the total current by the cross sectional area of the protrusion and need not match FEM values. The temperature was held constant at 300 K. Note that after about 11 GV/m, the GTFE (and also FN) equations are not valid.

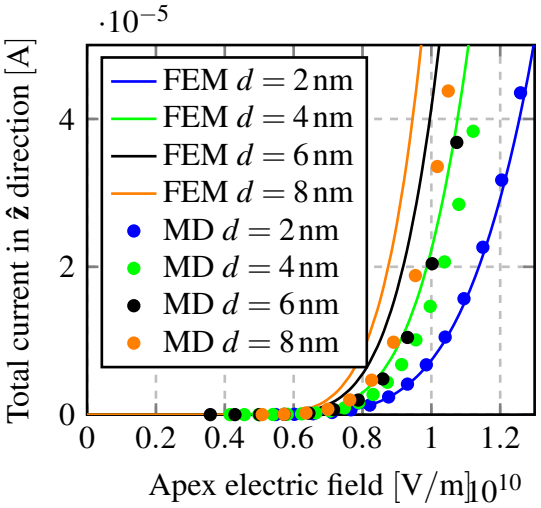

Figure 8: The total current in the $\hat{\mathbf{z}}$ direction versus the apex electric field for FEM and MD. Protrusion is a cylinder with hemispherical cap, height is constant at $h = 5\,\text{nm}$. The temperature is held constant at 300 K. Note that after about 11 GV/m, the GTFE (and also FN) equations are not valid.

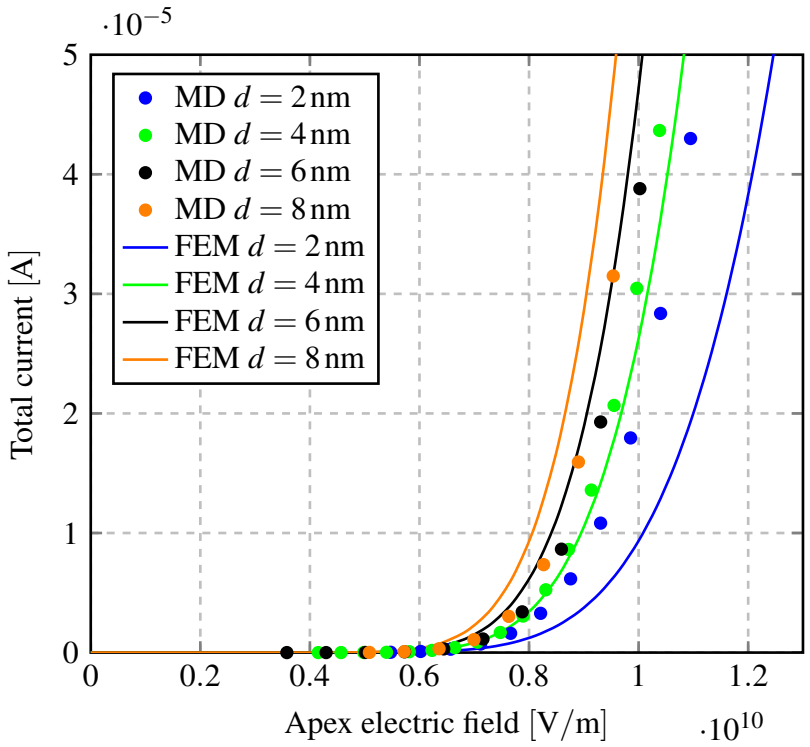

Figure 9: The total current from the emitter versus the apex electric field for FEM and MD. Protrusion is a cylinder with hemispherical cap, height is constant at $h = 5\,\mathrm{nm}$. FEM calculations used the mesh described in table 1. The temperature is held constant at 300 K. Note that after about 11 GV/m, the GTFE (and also FN) equations are not valid.

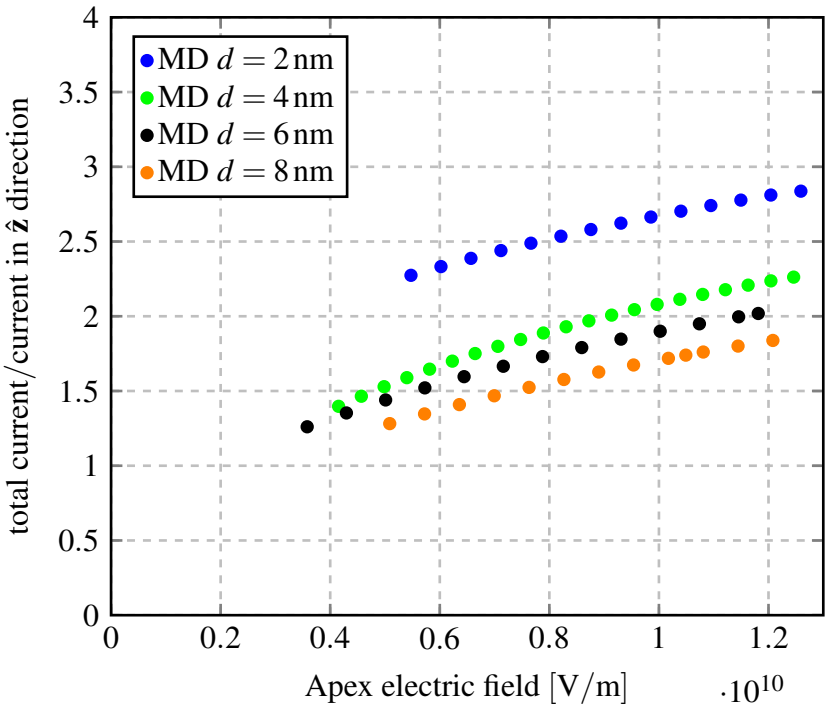

Figure 10: The ratio of MD values from two previous figures (8 and 9).

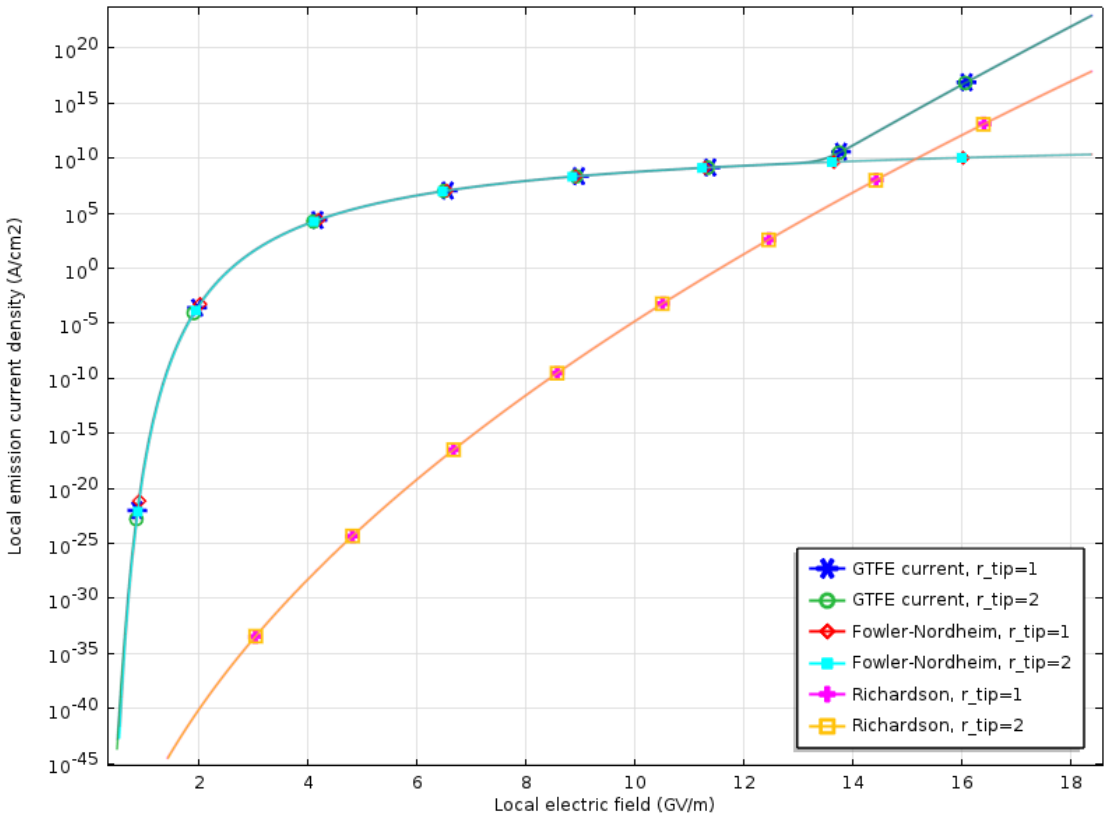

Figure 11: The current density dependence on local electric field. The temperature is held constant at 300 K. Note that after about 11 GV/m, the GTFE (and also FN) equations are not valid.

4 Various results for constant temperature $T_0 = 1000\,\mathrm{K}$

Note: The apex values found in this section do not correspond to the real apex point, but a point in close proximity. This is due to the COMSOL solver not finding the field correctly in the real apex point (and the values are unrealistic). The deviation in the used point from the real apex field is less than 0.2 %.

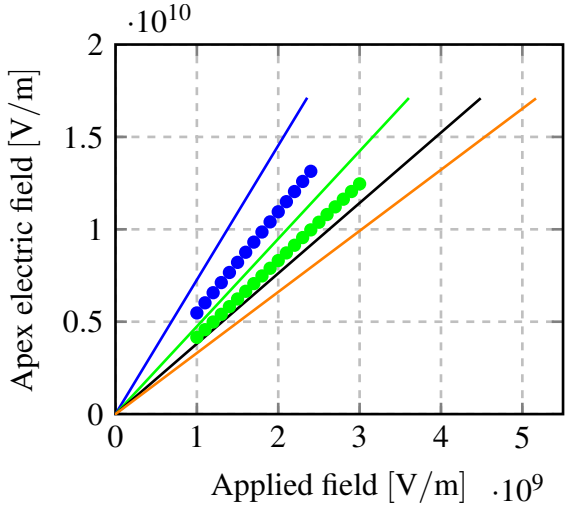

(a) Apex electric field

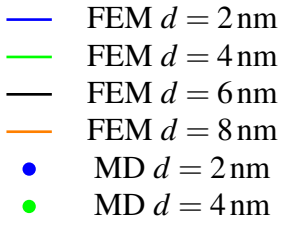

(b) Legend

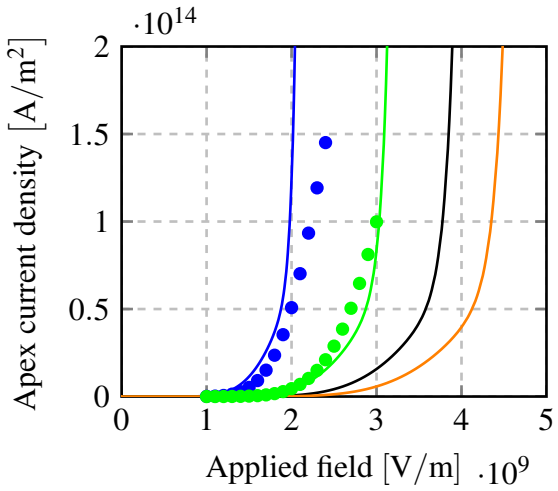

(c) Apex current density (indirect case for MD)

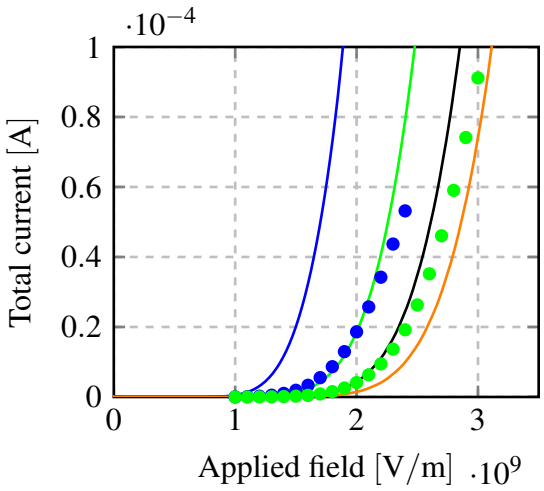

(d) Total current from emitter

Figure 12: The local apex electric field (a), local apex (GTFE) current density (c) and the total current (d) dependence on applied electric field. Each of the dependences have been found for two protrusion sizes: ($h = 5\,\mathrm{nm}$, $d = 2\,\mathrm{nm}$) and ($h = 5\,\mathrm{nm}$, $d = 4\,\mathrm{nm}$). The dependencies have been found with weak constraints enabled (for the Diriclet boundary condition of potential on copper surface). The temperature was held constant at $T_0 = 1000\,\mathrm{K}$. The used mesh was the same as in table 1.

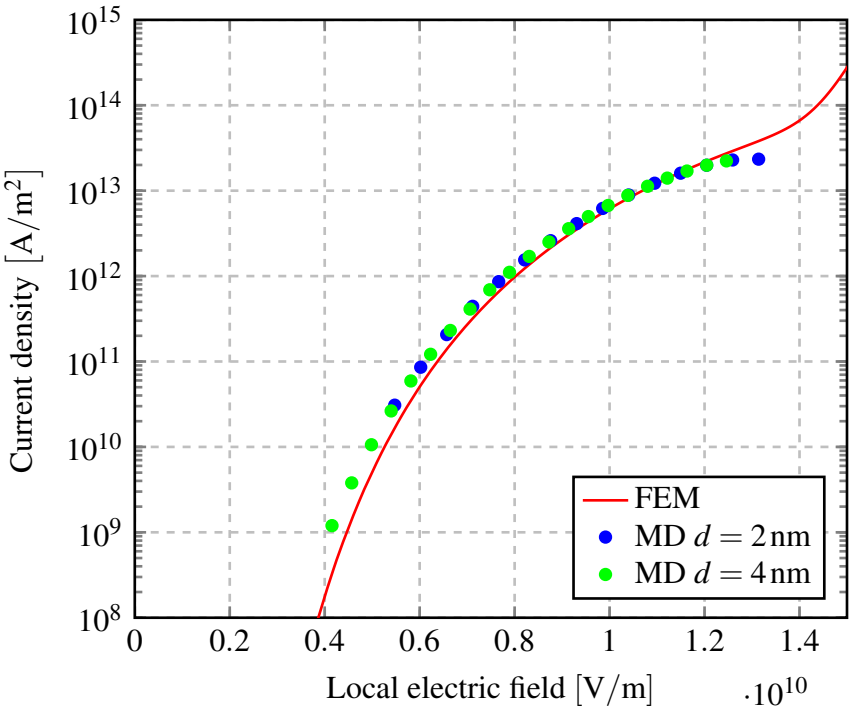

Figure 13: The current density dependence on local electric field for FEM and MD. The values for MD current density has been found indirectly and need not match FEM values. The temperature was held constant at 1000 K. Note that after about 11 GV/m, the GTFE (and also FN) equations are not valid. Difference between direct MD and FEM, (see also in ymode = log).

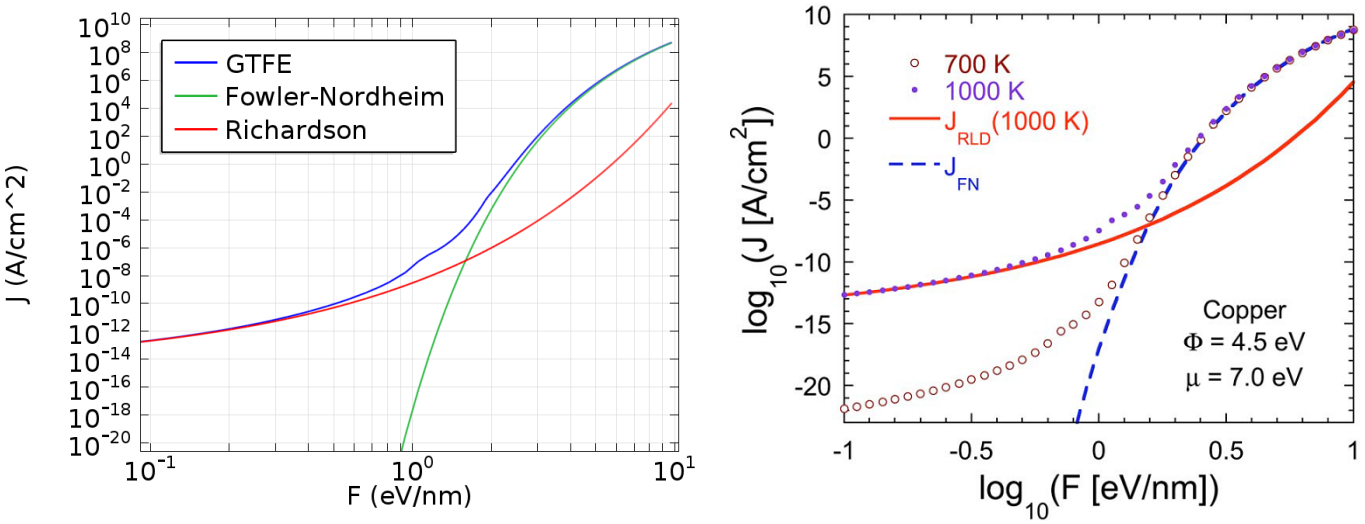

Figure 14: Current density dependence on local electric field on a constant ($T_0 = 1000K$) temperature. The graph on the left shows my implementation in COMSOL, and on the right is the Jensen's implementation (taken from Kevin L Jensen. "General formulation of thermal, field, and photoinduced electron emission" (2007))

5 Electric field and potential for a flat surface

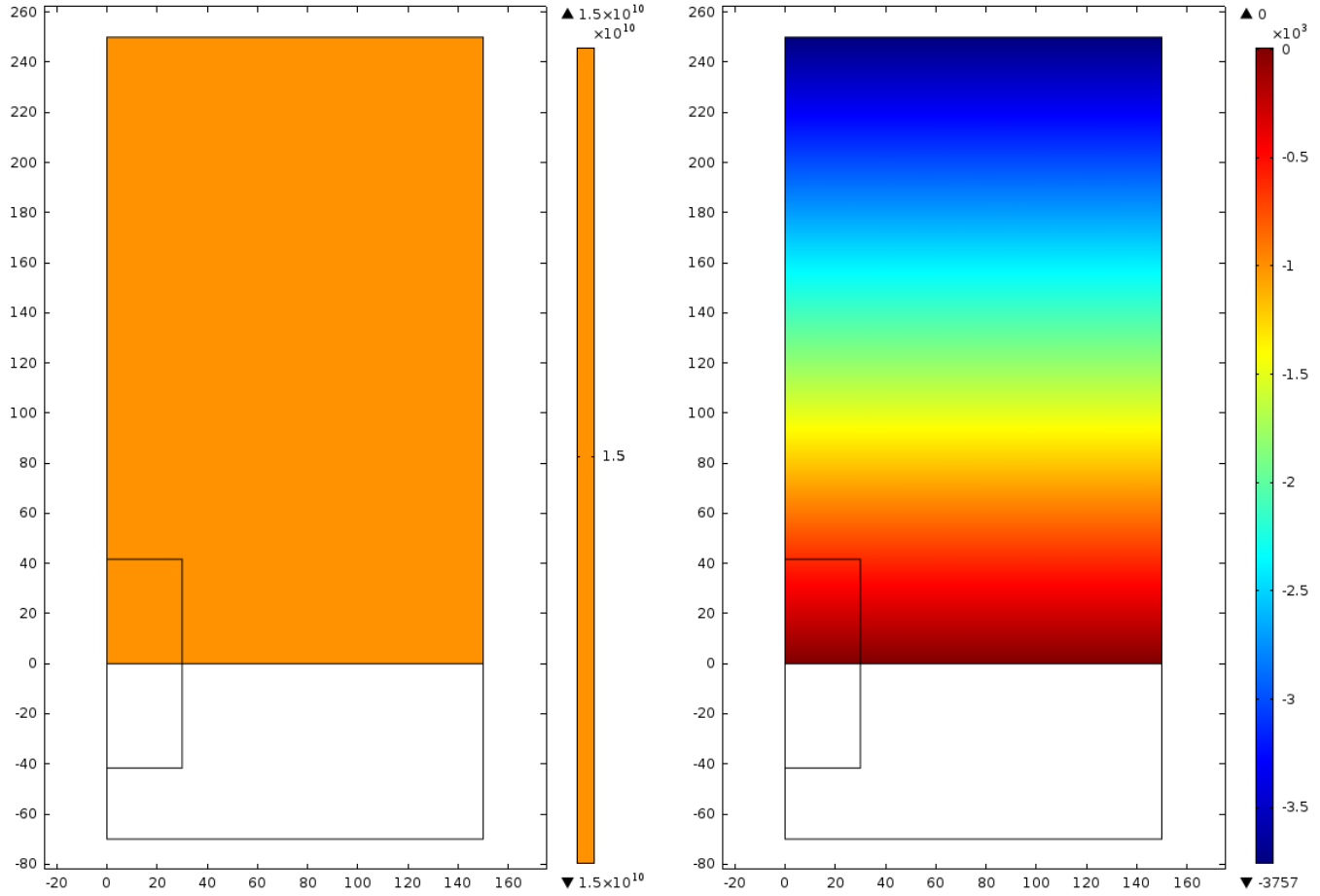

Figure 15: The electric field norm value in $[\mathrm{V/m}]$ (left) and the electric potential in $[\mathrm{V}]$ (right). The positional values are in nanometers. The applied electric field was $1.503 \times 10^{10}\,\mathrm{V/m}$. The used mesh was uniform and coarse (element length was about 10 nm).

6 Total current from protrusion for equilibrium temperature; comparison of MD and FEM

Note: All FEM currents have been calculated from the whole copper boundary (as opposed to only the tip in MD). In high field conditions ($> 0.01 \frac{V}{nm}$) the tip currents make up more than 99.97% of the total surface current.

6.1 Non-uniform fine mesh

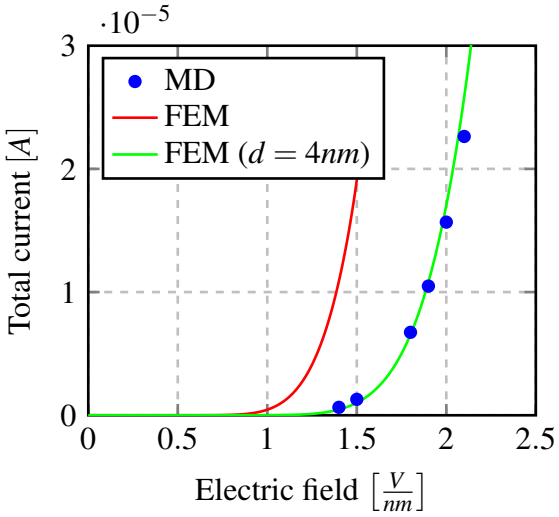

(a) $h = 5nm, d = 2nm, \beta \approx 2.5$

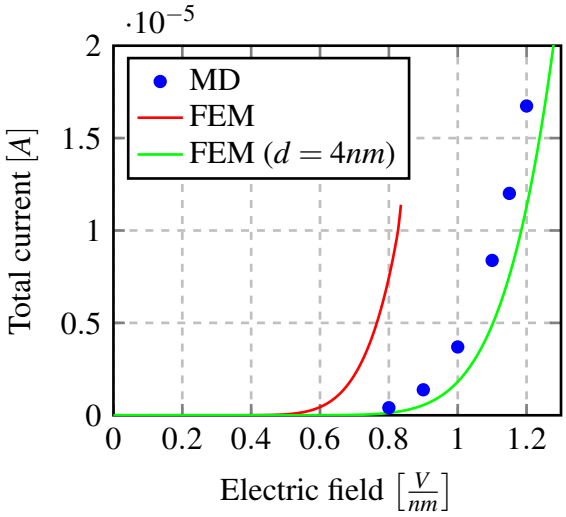

(b) $h = 10nm, d = 2nm, \beta \approx 5$

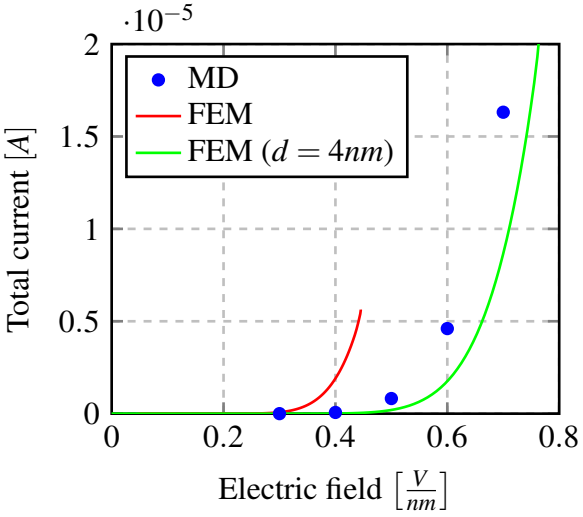

(c) $h = 20nm, d = 2nm, \beta \approx 10$

Figure 16: Total general thermal field emission current from protrusions dependence on applied field for MD and FEM simulations. The temperature develops due to equilibrium of resistive heating and thermal conduction. The mesh parameters are given in table 1.Note that the local electric field dependence on the applied field is different for MD and FEM. Also MD calculates only the total current in Z direction.

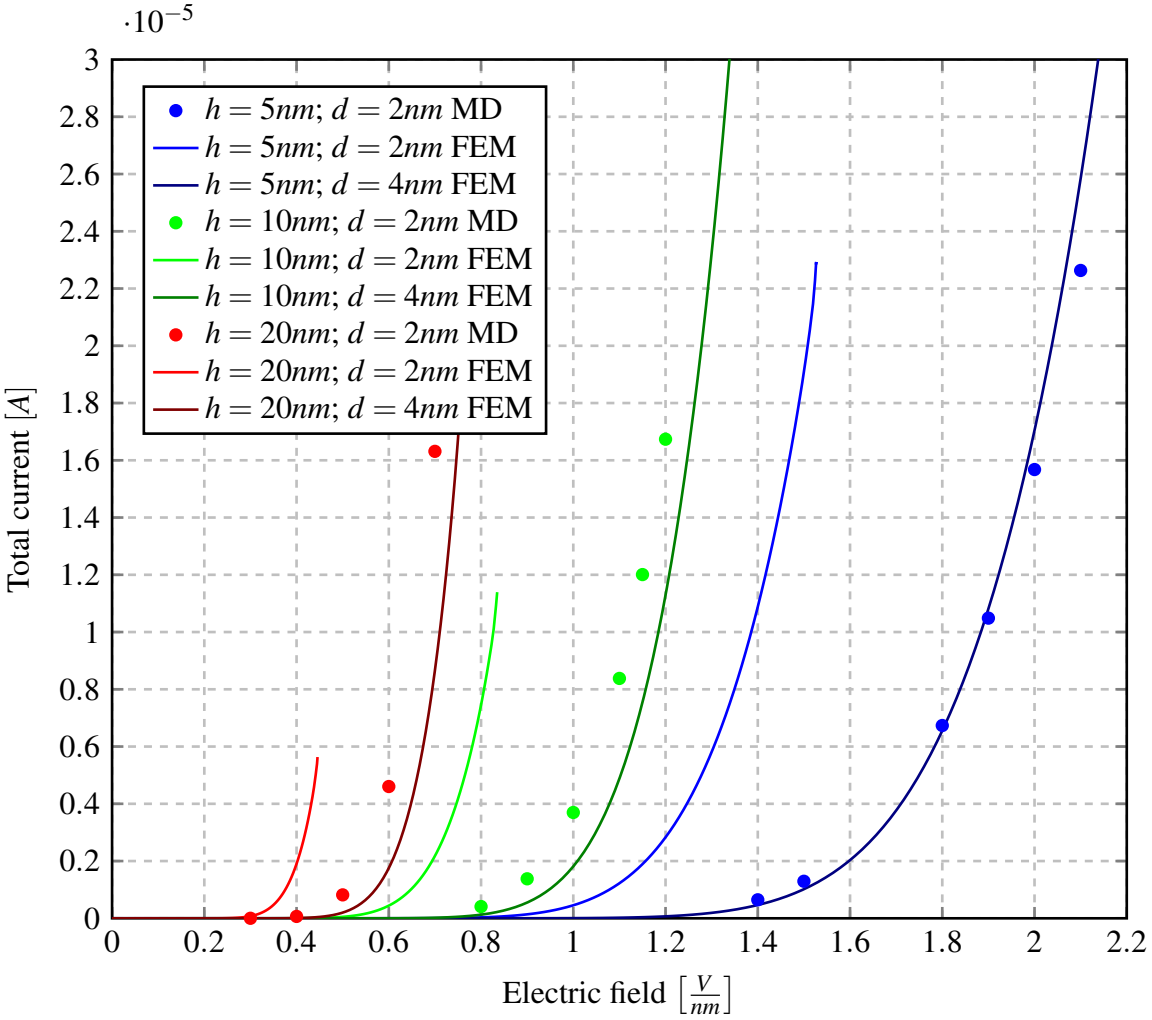

Figure 17: The data from figure 16 on one plot.

Maximum element size	$1.8nm$
Minimum element size	$0.0004nm$
Maximum element growth rate	1.2
Curvature factor	0.001
Resolution of narrow regions	3

Table 1: Mesh parameters for figures 16 and 17

6.2 Uniform triangular mesh

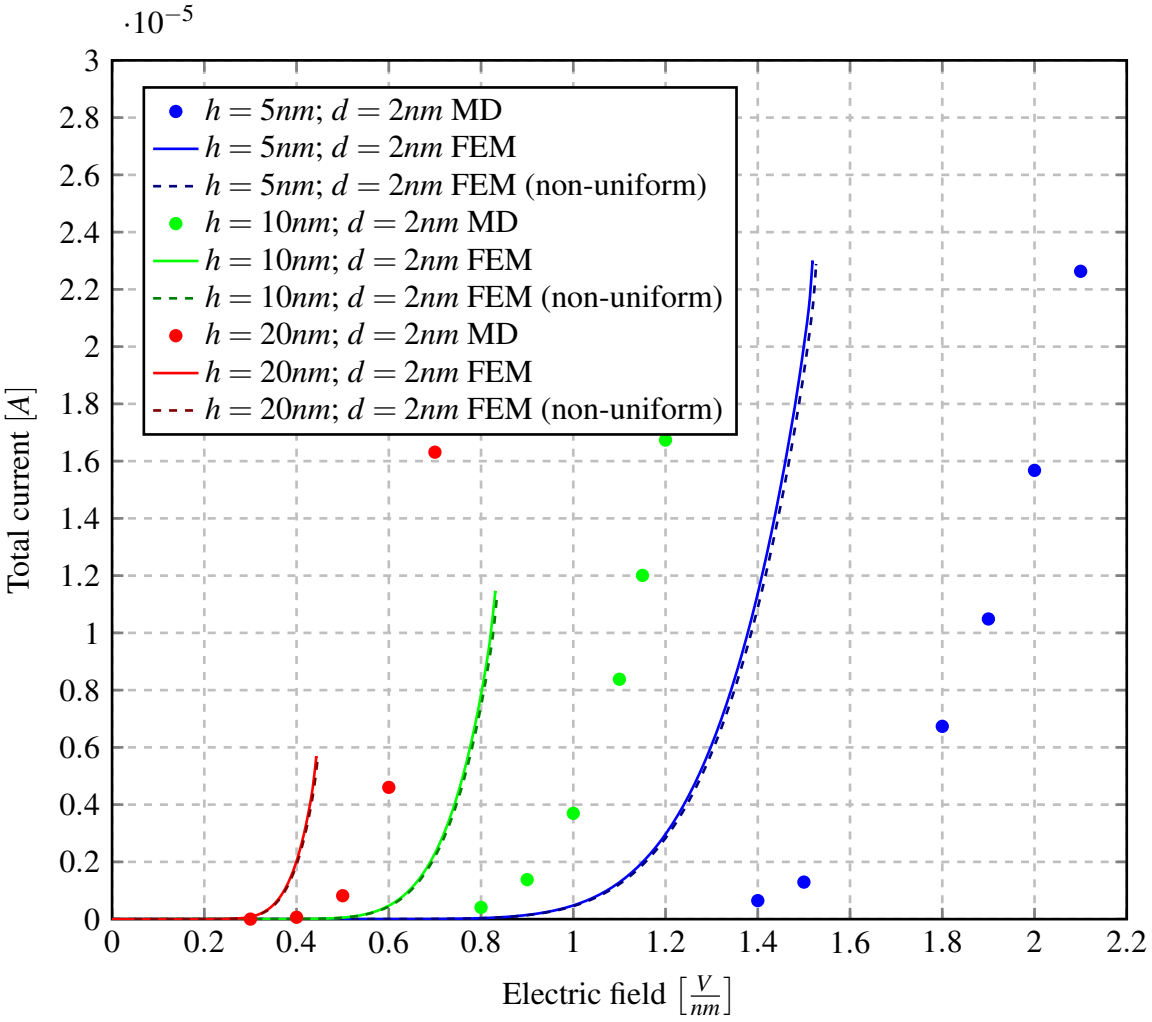

Figure 18: Total general thermal field emission current from protrusions dependence on applied field for MD and FEM simulations. It includes the FEM results of both the uniform triangular mesh (see figure 19) and the non-uniform mesh (see table 1).

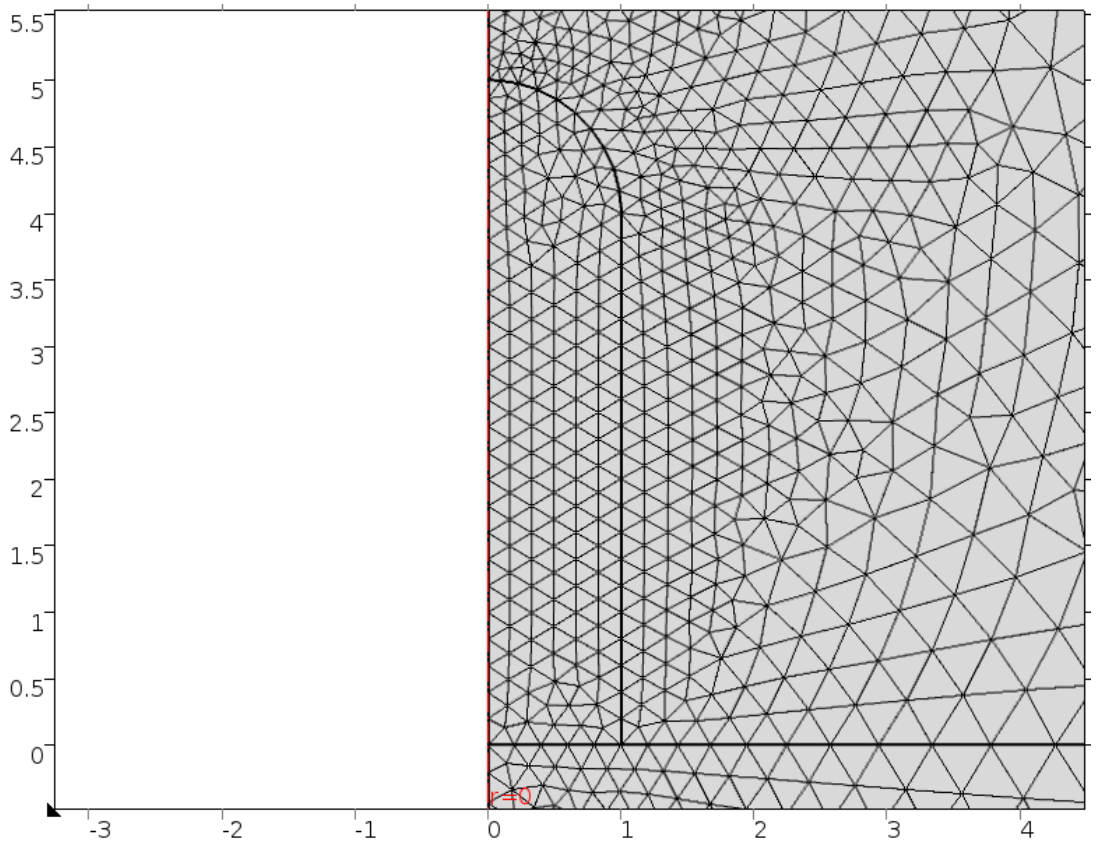

Figure 19: The protrusion has an uniform triangular mesh, where each element's size is $0.2nm$.

7 Total current from protrusion for equilibrium temperature

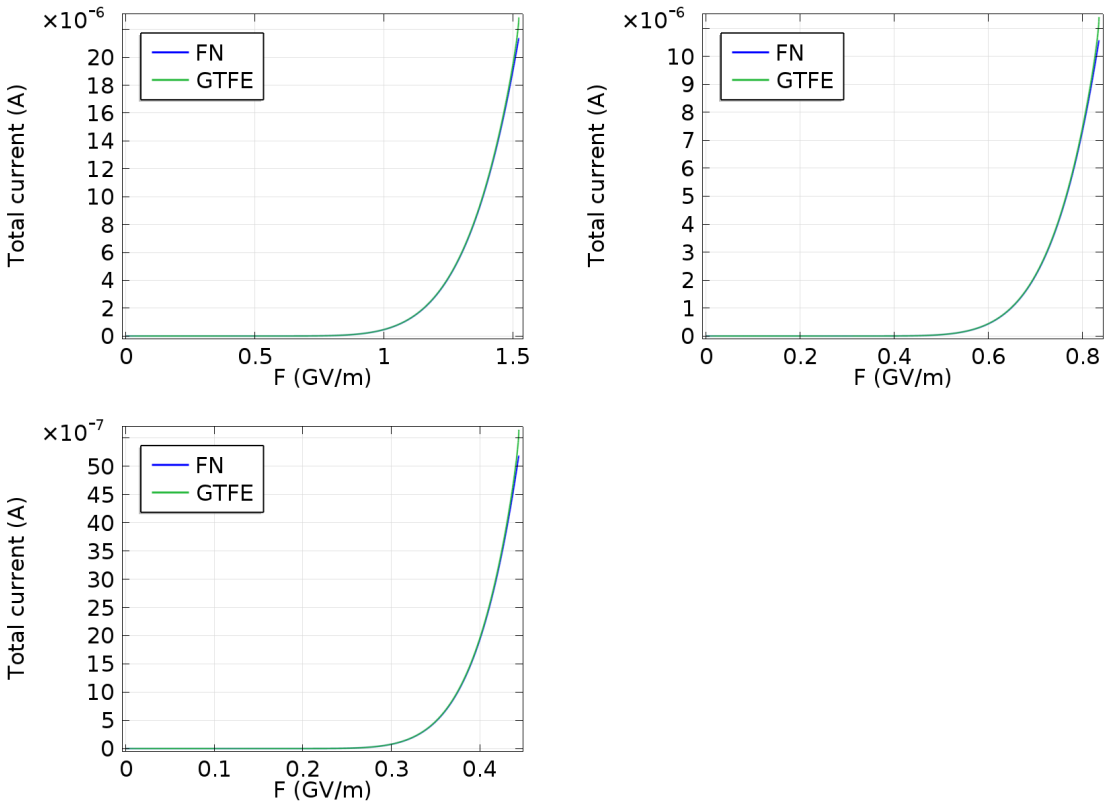

Figure 20: Total general thermal field emission current from protrusions dependence on applied field. The temperature develops due to equilibrium of resistive heating and thermal conduction (nano scale size effects are taken into account). Upper left: $h = 5nm, d = 2nm, \beta \approx 2.5$; upper right: $h = 10nm, d = 2nm, \beta \approx 5$; lower left: $h = 20nm, d = 2nm, \beta \approx 10$.

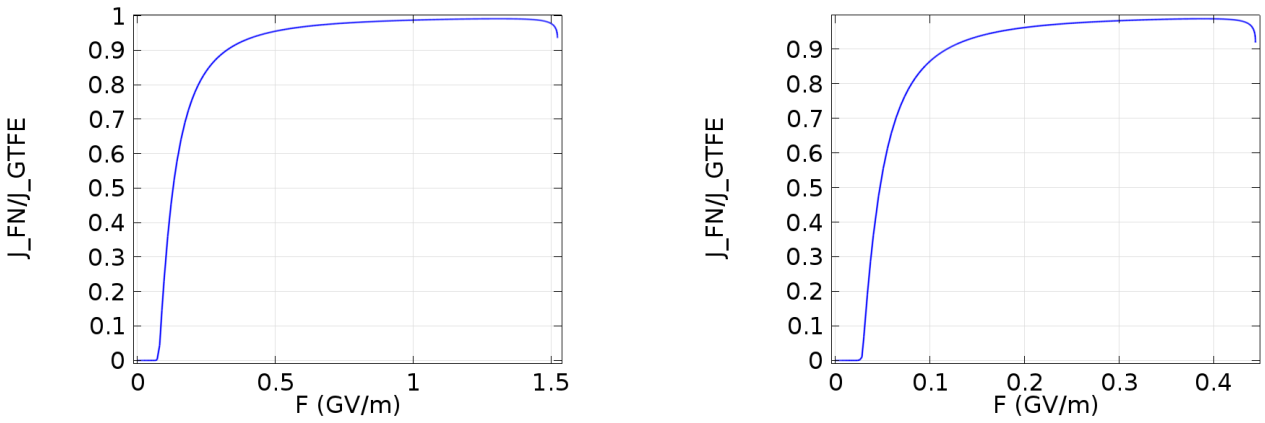

(a) $h = 5nm, d = 2nm, \beta \approx 2.5$ **(b)** $h = 20nm, d = 2nm, \beta \approx 10$

Figure 21: The total integrated Fowler-Nordheim current's ratio to the general thermal field current. Same conditions as in figure 20.

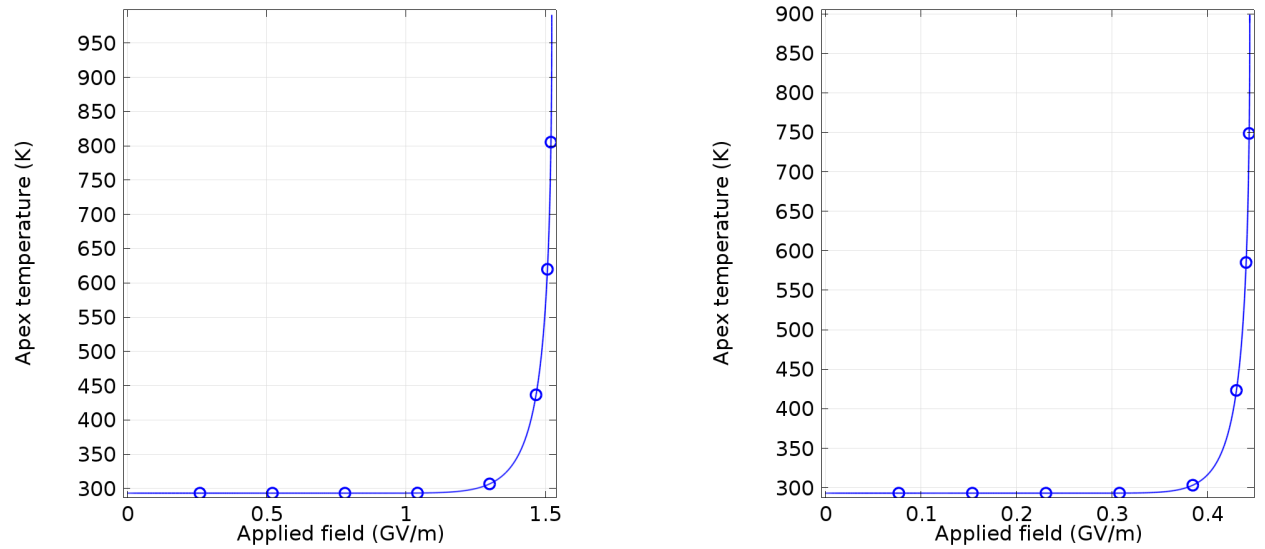

(a) $h = 5nm, d = 2nm, \beta \approx 2.5$ **(b)** $h = 20nm, d = 2nm, \beta \approx 10$

Figure 22: Apex temperature dependence on the applied field. Same conditions as in figure 20.

8 Total current from protrusion for constant temperature $T_0 = 1200K$

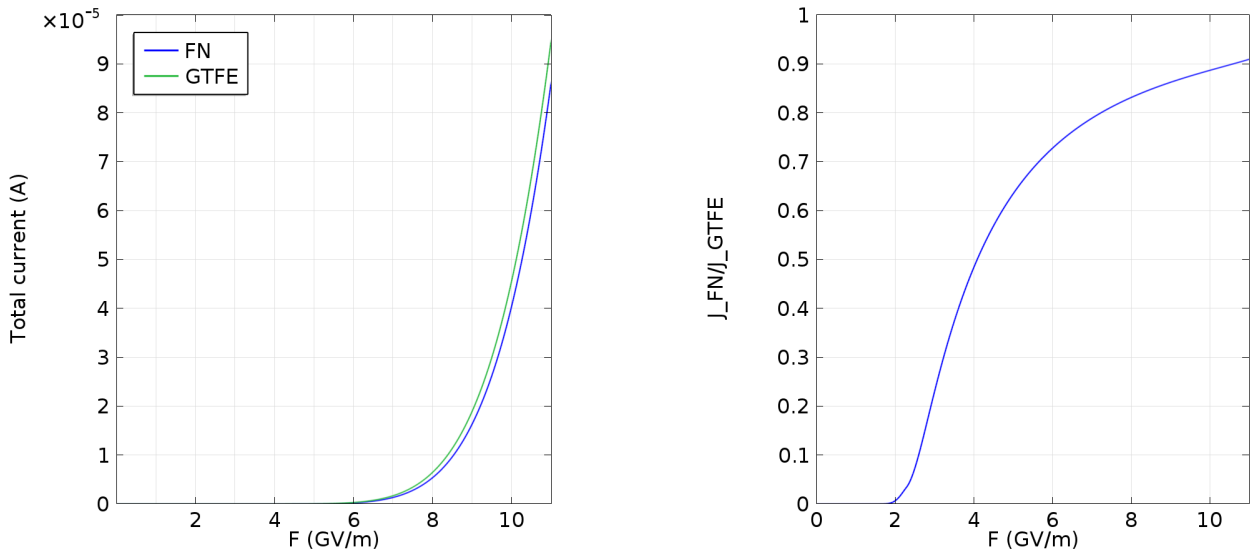

Figure 23: Total current (left) and the Fowler-Nordheim current ratio to the general thermal field current (right) dependence on the external applied field. Temperature is held constant at $T_0 = 1200K$ and the protrusion's dimensions are $h = 10nm, d = 2nm, \beta \approx 5$.